Relationships between bridging oxygen ^{17}O quadrupolar coupling parameters and structure in alkali silicates

Karl E. Vermillion, Pierre Florian,[a] and Philip J. Grandinetti[b]
Department of Chemistry, The Ohio State University, Columbus, Ohio 43210-1173

(Received 1 December 1997; accepted 27 January 1998)

We have performed *ab initio* calculations on the model cluster $(OH)_3Si–O–Si(OH)_3$ with lithium or sodium cations coordinated to the central oxygen in order to refine the relationships between ^{17}O quadrupolar coupling parameters and the local structure around the bridging oxygen in the case of alkali silicates. We have also used a point charge model to derive approximate expressions to describe the dependence of the ^{17}O electric field gradient tensor on the orientation of the alkali cation-bridging oxygen internuclear vector(s). From these calculations we predict that the previously established trend in ^{17}O quadrupolar coupling constant, C_q, with Si–O–Si angle is systematically shifted to lower magnitudes with increasing number and field strength of coordinating alkali cations and that C_q will be relatively insensitive to variations in the alkali cation-bridging oxygen internuclear vector orientation. The previously established trend in ^{17}O quadrupolar coupling asymmetry parameter, η_q, with Si–O–Si angle is systematically shifted to higher values by the presence of one coordinating alkali cation, and only slightly shifted to higher values by the presence of two coordinating alkali cations. As with the quadrupolar coupling constant, the magnitude of the shift in asymmetry parameter increases with increasing field strength of the coordinating alkali cation(s). In contrast to C_q, η_q is additionally dependent on variations in the alkali cation-bridging oxygen internuclear vector orientation. With two or more coordinating alkali cations, however, the magnitude of these variations are reduced, and for certain alkali cation configurations are eliminated. Finally, the parametric dependence of C_q on η_q via the Si–O–Si angle can be used to distinguish between bridging oxygen environments with differing number of coordinating alkali cations. © *1998 American Institute of Physics.* [S0021-9606(98)01217-3]

I. INTRODUCTION

The potential of oxygen-17 solid-state nuclear magnetic resonance (NMR) as a probe of structure in solids has been greatly enhanced with the recent development of solid-state NMR techniques such as double rotation (DOR),[1] dynamic-angle spinning (DAS),[2–5] and multiple-quantum magic-angle spinning (MQ-MAS)[6] which provide high-resolution NMR spectra of quadrupolar nuclei in solids. Because of the historical difficulties associated with doing ^{17}O solid-state NMR, however, relatively little is known of the relationships between ^{17}O NMR parameters and structure when compared to the more commonly used spin 1/2 probes such as ^{13}C, ^{29}Si, or ^{31}P. Tossell and co-workers[7–9] have shown that *ab initio* quantum chemical calculations can be a powerful tool for researchers trying to connect measured ^{17}O NMR parameters to structural features. Indeed, the Tossell group's *ab initio* predicted trends[7–9] in ^{17}O quadrupolar coupling parameters with Si–O–Si bond angle have been experimentally verified using ^{17}O DAS,[10] and these theoretically derived trends have been indispensable in quantifying structural distributions in silicate glasses.[11]

As we have applied ^{17}O DAS to an increasing number of silicate systems we have noticed that the trends in ^{17}O quadrupolar coupling constant with Si–O–Si angle are slightly dependent on the presence of neighboring network modifying cations. This has been recently noted by Maekawa and co-workers[12] who had to adjust previous empirical relationships determined from silica polymorphs studies to account for their ^{17}O results on alkali silicates. To further understand this affect we have used *ab initio* methods to investigate how variations in the bridging oxygen ^{17}O quadrupolar coupling parameters in silicate clusters as a function of bridging oxygen angle are affected by the presence of one and two coordinating network modifying alkali cations, such as lithium or sodium. These results should provide insight to future researchers using ^{17}O solid-state NMR to study the structure of glasses and as well as other silicate-based materials such as zeolites.

II. THEORY AND CALCULATIONS

The quadrupolar Hamiltonian can be written in the form

$$H_Q = \sqrt{\frac{3}{2}}\frac{eQ}{I(2I-1)}\sum_m (-1)^m R_{2,m} T_{2,-m}, \tag{1}$$

where I is the nuclear spin, Q is the nuclear electric quadrupole moment, and $T_{2,m}$ are irreducible spherical tensor operators describing the nuclear spin state. The electric field gradient (efg) due to surrounding electrons and nuclei is de-

[a]Current address: CNRS-CRPHT, 1D Av. de la Recherche Scientifique, 45071 Orléans Cedex 2, France.
[b]Author to whom correspondence should be addressed.

scribed by the irreducible spherical tensor operators $R_{2,m}$, and can be written as the sum over all electrons and nuclei surrounding the nucleus of interest, that is

$$R_{2,m}=\sum_{\text{all electrons}} E_{2,m}+\sum_{\text{all nuclei}} N_{2,m}, \tag{2}$$

where

$$E_{2,m}=-e\sqrt{\frac{4\pi}{5}}\,\frac{1}{r_e^3}Y_{2,m}(\theta_e,\phi_e), \tag{3}$$

$$N_{2m}=Z_n e\sqrt{\frac{4\pi}{5}}\,\frac{1}{r_n^3}Y_{2,m}(\theta_n,\phi_n), \tag{4}$$

and r_e, θ_e, ϕ_e and r_n, θ_n, ϕ_n describe the distance and orientation of the surrounding electrons and nuclei, respectively, with respect to the nucleus of interest. When written in its principal axis system (PAS) the expectation value of the efg is related to the quadrupolar coupling constant and asymmetry parameter according to

$$C_q=2\frac{eQ}{h}\langle\rho_{2,0}\rangle \quad \text{and} \quad \eta_q C_q=2\sqrt{6}\,\frac{eQ}{h}\langle\rho_{2,\pm 2}\rangle, \tag{5}$$

where $\langle\rho_{2,m}\rangle$ is the expectation value of the irreducible spherical tensor elements of the efg in its PAS.[13] The expectation value for $R_{2,m}$ is calculated using Eqs. (2)–(4) and the wavefunction for the system.

A. *Ab initio* calculations

Ab initio calculations were performed on a Silicon Graphics PowerIndigo-2 workstation using GAUSSIAN 94 (Ref. 14) at a restricted Hartree–Fock level with a 6-31 +G(d) basis set. GAUSSIAN 94 calculates the traceless efg tensor and outputs its cartesian tensor elements. These calculated efg tensor elements are related to the quadrupolar coupling constant, C_q, and quadrupolar coupling asymmetry parameter, η_q, according to

$$C_q=e^2Q\langle q_{zz}\rangle/h, \quad \text{and} \quad \eta_q=\frac{\langle q_{xx}\rangle-\langle q_{yy}\rangle}{\langle q_{zz}\rangle}, \tag{6}$$

where $e\langle q_{xx}\rangle$, $e\langle q_{yy}\rangle$, and $e\langle q_{zz}\rangle$ are the principal components of the electric field gradient tensor defined such that

$$|\langle q_{zz}\rangle|>|\langle q_{yy}\rangle|>|\langle q_{xx}\rangle|. \tag{7}$$

Inverting Eq. (6) we obtain

$$\begin{aligned}\frac{e^2Q}{h}\langle q_{xx}\rangle&=-\frac{1}{2}C_q(1-\eta_q),\\ \frac{e^2Q}{h}\langle q_{yy}\rangle&=-\frac{1}{2}C_q(1+\eta_q),\\ \frac{e^2Q}{h}\langle q_{zz}\rangle&=C_q.\end{aligned} \tag{8}$$

For ^{17}O a value of $e^2Q/h=-6.11$ MHz a.u.[3] was used to convert the q_{zz} output from Gaussian into the ^{17}O quadrupolar coupling constant. The sign of the quadrupolar coupling constant C_q was determined to be negative in all calculated cases. Generally it is more difficult to measure the sign of C_q than its magnitude, therefore only $|C_q|$ is often reported in the literature.

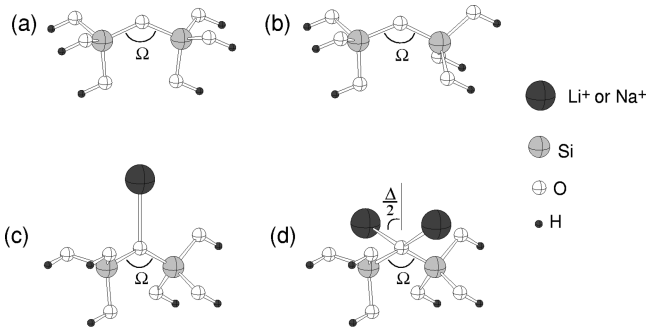

FIG. 1. Four molecular geometries used to investigate the effect of coordinating network modifying cations such as Li^+ and Na^+ near the bridging oxygen on its ^{17}O quadrupolar coupling parameters. (a) Eclipsed configuration, (b) staggered configuration, (c) staggered configuration with one modifier cation in the plane of the Si–O–Si angle and in the plane that bisects the Si–O–Si angle, and (d) staggered configuration with two modifier cations in the plane that bisects the Si–O–Si angle and each at an angle $\pm\Delta/2$, respectively, away from the plane of the Si–O–Si angle.

The three model clusters chosen to represent the bridging oxygen environment were (1) $(OH)_3Si–O–Si(OH)_3$, (2) $M[(OH)_3Si–O–Si(OH)_3]$, and (3) $M_2[(OH)_3Si–O–Si(OH)_3]$ where $M=Li^+$ or Na^+. See Fig. 1 for a graphical representation of the various clusters. These clusters were designed to mimic fragments commonly observed in a number of network modified crystalline alkali silicates. Other alkali were not investigated due to limitations of our 6-31+G(d) basis set.

B. Point charge model

If as a first approximation the modifier cations are treated as point charges then the efg at the bridging oxygen should vary according to

$$\begin{aligned}\langle R_{2,m}(\Omega)\rangle=&\langle\rho_{2,m}^{(\infty)}(\Omega)\rangle\\ &+(1-\gamma_\infty)\sum_j\frac{Z_j e}{d_j^3}\sqrt{\frac{4\pi}{5}}Y_{2,m}(\theta_j,\phi_j),\end{aligned} \tag{9}$$

where $\rho_{2,m}^{(\infty)}(\Omega)$ are the efg tensor elements of the bridging oxygen in the absence of the modifier cation, Ω is the Si–O–Si angle of the cluster, γ_∞ is the Sternheimer anti-shielding factor for the bridging oxygen, Z_j is the modifier cation charge, d_j is the distance between each alkali cation and the bridging oxygen, and (θ_j,ϕ_j) are the angles between each oxygen-cation internuclear vector and the bridging oxygen efg PAS in the absence (i.e., $d=\infty$) of the modifier cation (see Fig. 2).

The Sternheimer anti-shielding factor γ_∞ takes into account the efg induced near the bridging oxygen when the wavefunction of the cluster molecule is perturbed by a distant point charge(s).[15,16] This induced efg is in addition to the efg produced by the point charge itself and is predicted to be proportional to the efg produced by the point charge. While the Sternheimer anti-shielding factor is predicted in the context of the spherically symmetric electron distribution of an

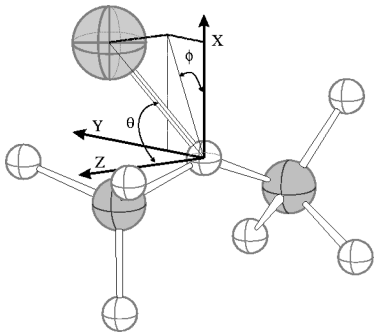

FIG. 2. Orientation of the coordinating alkali cation with respect to the original (i.e., $d=\infty$) bridging oxygen ^{17}O efg principal axis system.

atom or monoatomic ion the same effect would still be present in the asymmetric electron distribution of a molecule. In the molecular case, however, we cannot expect the anti-shielding factor on an atom in the molecule to be independent of either molecular configuration or the orientation of the external point charge(s) with respect to the molecule. Exploring this configuration and orientation dependence is beyond the scope of this article and its behavior is not necessarily pertinent to our discussion and conclusions. Nonetheless, we include a scalar Sternheimer anti-shielding factor in our point charge model as an adjustable parameter necessary to achieve agreement with our *ab initio* predicted results.

In all of our *ab initio* calculations except one, the z-axis of efg PAS remains the same as for $\rho^{(\infty)}_{2,m}(\Omega)$. Thus as a first approximation we neglect the $R_{2,\pm1}(\Omega)$ tensor elements of Eq. (9) for small deviations of θ away from 90°. Assuming also that the efg PAS z-axis assignment is unchanged by the presence of external point charges we define

$$C_q(\Omega)\approx 2\frac{eQ}{h}\langle R_{2,0}(\Omega)\rangle. \tag{10}$$

We cannot assume, however, that the orientation of the x- and y-axes of the efg PAS remains the same as for $\rho^{(\infty)}_{2,m}(\Omega)$, or even that the handedness of the coordinate system remains the same. Thus we assume that the final efg tensor will be block diagonal in the original efg PAS, and after diagonalizing this block-diagonal efg tensor we obtain

$$\eta_q C_q=\sqrt{6}\,\frac{eQ}{h}\sqrt{(\langle R_{2,2}\rangle+\langle R_{2,-2}\rangle)^2-(\langle R_{2,-2}\rangle-\langle R_{2,2}\rangle)^2}, \tag{11}$$

and

$$\tan 2\alpha = i\cdot\frac{\langle R_{2,-2}\rangle-\langle R_{2,2}\rangle}{\langle R_{2,2}\rangle+\langle R_{2,-2}\rangle}, \tag{12}$$

where α is the rotation in the original efg PAS about the z-axis from the x-axis to the new efg PAS x-axis assuming there were no changes in the handedness of the coordinate system. Changes in the handedness occur when $|\langle q_{xx}\rangle| > |\langle q_{yy}\rangle|$. This can be determined by substituting the results of Eqs. (10) and (11) into Eq. (8). In this situation, the efg PAS axes system is redefined, and, if necessary, the η_q value obtained from Eq. (11) is redefined as positive.

While one might expect that the approximations leading to Eqs. (10)-(12) would breakdown on close approach where substantial orbital interactions between alkali and bridging oxygen occur, we shall see that these expressions can still provide a qualitative and a certain degree of quantitative understanding of the trends we observe.

III. RESULTS AND DISCUSSION

A. The $(OH)_3Si-O-Si(OH)_3$ cluster

For the eclipsed and staggered configurations and a fixed ∠Si–O–Si, the d(Si–O) and d(O–H) distances (identical for all O, Si and H) were optimized with an STO-3G basis set. These results then served as the input for a final optimization with a 6-31+G(d) basis set. The final parameters as a function of ∠Si–O–Si are given in Table I.

The optimized geometry of the $(OH)_3Si-O-Si(OH)_3$ molecule shows a tendency to decrease the Si–O distance as ∠Si–O–Si increased, which is consistent with what has been observed in crystalline silicates.[17] At high Si–O–Si angles, however, the calculated energy differences are quite small and susceptible to basis set effects. Therefore, one

TABLE I. ^{17}O quadrupolar coupling parameters, distances, and relative energies obtained from *ab initio* calculations on the $(OH)_3Si-O-Si(OH)_3$ molecule in staggered and eclipsed configurations. The d(O–H) distance remained constant at 0.949 Å at all Si–O–Si angles. The euler angles α_q, β_q, and γ_q give the orientation of the efg PAS with respect to a molecular frame with the x- and z-axes lying in the plane of the Si–O–Si angle with the z-axis perpendicular to the bisector of the Si–O–Si angle. α_q and γ_q were identically zero at all Si–O–Si angles. The energies are referenced with respect to the staggered cluster with a Si–O–Si angle of 180°.

Staggered						Eclipsed				
∠Si–O–Si (deg)	d(Si–O) (Å)	Energy (kJ/mol)	C_q (MHz)	η_q	β_q (deg)	d(Si–O) (Å)	Energy (kJ/mol)	C_q (MHz)	η_q	β_q (deg)
120°	1.641	24.92	−5.04	0.718	−0.44°	1.6475	75.13	−5.06	0.692	0.0°
130°	1.638	9.53	−5.67	0.441	−0.23°	1.6395	23.43	−5.66	0.408	0.0°
140°	1.636	3.43	−6.17	0.260	−0.13°	1.6364	8.33	−6.16	0.232	0.0°
150°	1.635	1.22	−6.54	0.139	−0.07°	1.6347	3.57	−6.53	0.118	0.0°
160°	1.634	0.54	−6.78	0.059	−0.03°	1.6335	1.94	−6.77	0.046	0.0°
170°	1.633	0.18	−6.92	0.015	−0.01°	1.6327	1.21	−6.91	0.008	0.0°
180°	1.632	0.00	−6.97	0.000	0.00°	1.6324	0.94	−6.96	0.000	0.0°

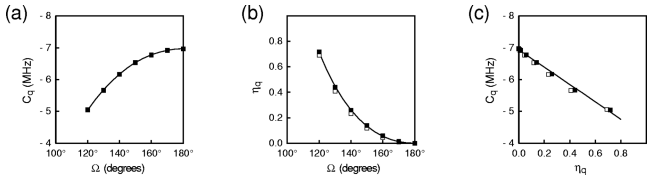

FIG. 3. *Ab initio* predicted values in (a) the ^{17}O quadrupolar coupling constant, C_q, (b) the ^{17}O quadrupolar asymmetry parameter, η_q, and (c) the correlation between C_q and η_q for the bridging oxygen in the $(OH)_3Si–O–Si(OH)_3$ molecule as a function of the Si–O–Si angle. The staggered configuration is shown as filled squares and the eclipsed configuration as open squares. Solid lines represent the best fit curves of Eqs. (13)–(14) through the staggered configuration *ab initio* data.

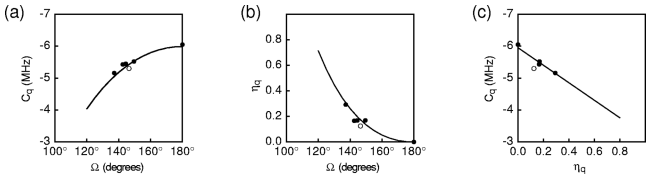

FIG. 4. Comparison of experimental data (symbols) and *ab initio* trends (solid lines) in (a) the ^{17}O quadrupolar coupling constant, C_q, (*ab initio* shifted by 1.00 MHz); (b) the ^{17}O quadrupolar asymmetry parameter, η_q, and (c) the correlation between C_q and η_q for the bridging oxygen in the staggered $(OH)_3Si–O–Si(OH)_3$ molecule as a function of the Si–O–Si angle. The coesite data (Ref. 10) are as shown as filled circles and the cristobalite data (Ref. 18) as open circles. Solid lines represent the best fit curves of Eqs. (13)–(14) through the staggered configuration *ab initio* data.

should be careful not to infer that Si–O–Si bond angle distributions in silicate glasses derive from the energy surface of this cluster along the Si–O–Si bond angle coordinate. For example, in earlier *ab initio* work[17] using an STO-3G basis set the same cluster was determined to have an energy minimum near a Si–O–Si angle of 144°, in agreement with the histogram of Si–O–Si angles found in crystalline polymorphs of SiO_2. Based on our results at a higher basis set it appears that this agreement between the STO-3G results and the crystallography data is perhaps fortuitous. In addition, in the case of alkali-coordinated bridging oxygen, as we show later, the calculated energy differences between clusters with Si–O–Si angles between 140° and 180° are still on the order of 2 kJ/mol. Thus, we generally conclude that while the distribution of Si–O–Si angles may be affected by this local energy surface, particularly at low angles, it may be that variations in higher coordination sphere structures such as silicate ring size have a stronger effect on the Si–O–Si angle distribution.

In Figs. 3(a) and 3(b) is the dependence of the *ab initio* predicted ^{17}O C_q and η_q data for the bridging oxygen in the $(OH)_3Si–O–Si(OH)_3$ molecule as a function of Si–O–Si angle. Only minor differences in the ^{17}O NMR quadrupolar coupling parameters can be found between the staggered and eclipsed configurations. We observe an increase in the magnitude of C_q and a decrease of η_q with increasing Si–O–Si angle, as is expected from experimental data obtained on the SiO_2 polymorph cristobalite[18] and coesite[10] as well as from previous *ab initio* calculations on the $H_3Si–O–SiH_3$ molecule.[7–9] In addition, the orientation of the bridging oxygen efg PAS was found to have its x- and z-axes lying in the plane of the Si–O–Si angle with the z-axis perpendicular to the bisector of the Si–O–Si angle. This result is in agreement with previous theoretical[7–9] and experimental[19,10,18] results.

From a practical point of view it is useful to describe the dependence of C_q and η_q on the Si–O–Si angle with analytical expressions. In an earlier work[10] we used the semiempirical Townes–Dailey[20] approach to obtain analytical expressions that closely followed this dependence. Below are these expressions modified with parameterized exponents to obtain better agreement with the *ab initio* and experimental data:

$$C_q(\Omega) = a \cdot \left(\frac{1}{2} + \frac{\cos \Omega}{\cos \Omega - 1} \right)^{\alpha}, \quad \text{and}$$

$$\eta_q(\Omega) = b \cdot \left(\frac{1}{2} - \frac{\cos \Omega}{\cos \Omega - 1} \right)^{\beta}. \tag{13}$$

By no means are these expressions unique in their ability to describe these relationships, and other expressions have been used previously.[9,21,11] For the *ab initio* staggered configuration we obtain $a = -6.97$ MHz and $\alpha = 1.78$ for our C_q expression, and $b = 5.02$ and $\beta = 1.09$ for our η_q expression. As seen in Fig. 3, the curves from these analytical expressions describe the trends well. Since C_q and η_q are related parametrically via the Si–O–Si angle we have also plotted the correlation between *ab initio* predicted C_q and η_q data in Fig. 3(c). Based on the expressions above and their parameter values we would predict a nearly linear correlation of the form

$$C_q \approx a \cdot \left(1 - \frac{\alpha}{b} \eta_q \right). \tag{14}$$

Over the range of C_q and η_q values calculated this correlation appears to be very close to linear ($r^2 = 0.996$), with a slope of 2.7 MHz and an intercept of -7.0 MHz, in close agreement with the parameters derived from the individual fits of Eq. (13) to C_q and η_q.

Experimental values from SiO_2 polymorphs and the trends from the *ab initio* calculations (C_q shifted by 1.00 MHz) are shown in Fig. 4. Although the C_q magnitudes obtained from the *ab initio* calculations are higher than experimental values by 1 MHz, they reproduce the experimental trends well. In Fig. 4(c) is a plot of the correlation between the experimentally measured ^{17}O bridging oxygen C_q and η data which also shows good agreement with the predicted linear correlation.

B. The M[(OH)$_3$SiOSi(OH)$_3$] cluster where M=Li$^+$ and Na$^+$

The effect of a single coordinating alkali cation on the ^{17}O quadrupolar coupling parameters of the bridging oxygen was investigated using *ab initio* calculations by placing ei-

ther a Li^+ or Na^+ cation in the plane of the Si–O–Si angle and in the plane that bisects the Si–O–Si angle as shown in Fig. 1(c). For each Si–O–Si angle the *ab initio* optimized $(OH)_3Si–O–Si(OH)_3$ cluster geometry found in the absence of the alkali cation was used in the cluster containing the coordinating alkali cation.

Using the point charge model we can predict variations in C_q, η_q, and efg PAS orientation with cation-oxygen distance and internuclear vector orientation by inserting Eq. (9) into Eqs. (10)–(12) to obtain

$$C_q(\Omega,d,\theta)\approx C_q^{(\infty)}(\Omega)+\Delta C_q(d)\cdot(3\cos^2\theta-1), \tag{15}$$

$$\eta_q(\Omega,d,\theta,\phi)C_q(\Omega,d,\theta)\approx\sqrt{(3\Delta C_q(d)\sin^2\theta\cos 2\phi+\eta_q^{(\infty)}(\Omega)C_q^{(\infty)}(\Omega))^2+(3\Delta C_q(d)\sin^2\theta\sin 2\phi)^2} \tag{16}$$

and

$$\tan 2\alpha\approx\frac{3\Delta C_q(d)\cdot\sin^2\theta\sin 2\phi}{3\Delta C_q(d)\cdot\sin^2\theta\cos 2\phi+C_q^{(\infty)}(\Omega)\eta_q^{(\infty)}(\Omega)}, \tag{17}$$

where

$$\Delta C_q(d)=(1-\gamma_\infty)\frac{Ze^2Q}{h}\cdot\frac{1}{d^3}, \tag{18}$$

and $C_q^{(\infty)}(\Omega)$ and $\eta_q^{(\infty)}(\Omega)$ are the quadrupolar coupling constant and asymmetry parameter for the bridging oxygen at infinite cation separation. It is instructive to point out a few general trends based on Eqs. (15)–(17) and the assumptions leading to them:

(1) Equation (15) predicts that C_q is generally independent of ϕ, and with d held constant the trend in C_q with Ω is shifted by a constant times $(3\cos^2\theta-1)$.

(2) In the special case where $\eta_q^{(\infty)}(\Omega)=0$ (i.e., $\angle$Si–O–Si $=180°$) Eq. (16) yields

$$\eta_q(\Omega,d,\theta,\phi)\approx 3\left(\frac{\Delta C_q(d)}{C_q(\Omega,d,\theta)}\right)\sin^2\theta, \tag{19}$$

indicating that η_q also becomes generally independent of ϕ. In addition, Eq. (17) reduces to

$$\tan 2\alpha=\tan 2\phi, \tag{20}$$

indicating that the alkali-oxygen internuclear vector defines the direction of the x-axis of the efg PAS.

(3) If $\phi=0°$ or $90°$ then Eq. (16) yields

$$\eta_q(\Omega,d,\theta,\phi)\approx\eta_q^{(\infty)}(\Omega)\left(\frac{C_q^{(\infty)}(\Omega)}{C_q(\Omega,d,\theta)}\right)+3\left(\frac{\Delta C_q(d)}{C_q(\Omega,d,\theta)}\right)\sin^2\theta. \tag{21}$$

If we assume that the ratios $[C_q^{(\infty)}(\Omega)/C_q(\Omega,d,\theta)]$ and $[\Delta C_q(d)/C_q(\Omega,d,\theta)]$ are approximately constant as a function of Ω, then we would predict that the trend in η_q with Ω is simply scaled and shifted by a constant times $\sin^2\theta$.

(4) In the case where $\phi=0°$ and $\theta=90°$, as shown in Fig. 1(c), we obtain the following expressions from Eq. (8):

$$\frac{e^2Q}{h}\langle q_{xx}\rangle=\frac{e^2Q}{h}\langle q_{xx}\rangle^{(\infty)}+2\Delta C_q(d),$$

$$\frac{e^2Q}{h}\langle q_{yy}\rangle=\frac{e^2Q}{h}\langle q_{yy}\rangle^{(\infty)}-\Delta C_q(d), \tag{22}$$

$$\frac{e^2Q}{h}\langle q_{zz}\rangle=\frac{e^2Q}{h}\langle q_{zz}\rangle^{(\infty)}-\Delta C_q(d).$$

With $\theta=90°$ and $\phi=0°$ these equations predict that upon approach of the cation $\langle q_{zz}\rangle$ and $\langle q_{xx}\rangle$ decrease in magnitude while $\langle q_{yy}\rangle$ increases. Keep in mind that $\langle q_{xx}\rangle+\langle q_{yy}\rangle+\langle q_{zz}\rangle=0$, and that $|\langle q_{zz}\rangle|>|\langle q_{yy}\rangle|>|\langle q_{xx}\rangle|$. With decreasing cation-oxygen distance eventually the magnitude of the efg along the y-axis will exceed that along the z-axis and then $\langle q_{zz}\rangle$ will switch to lying along the y-axis of the original PAS system, i.e., perpendicular the cation-oxygen internuclear vector direction, and in the plane that is perpendicular to the Si–O–Si plane and bisects the Si–O–Si angle. For the two types of cations studied here only in the case of Li^+ at a Si–O–Si angle of 120° does this situation occur. As a point of reference for the Si–O–Si angle of 180° the values of $(e^2qQ/h)\langle q_{xx}\rangle^{(\infty)}$, $(e^2qQ/h)\langle q_{yy}\rangle^{(\infty)}$, and $(e^2qQ/h)\langle q_{zz}\rangle^{(\infty)}$ are approximately 3.5 MHz, 3.5 MHz, and -7.0 MHz, respectively. For a coordinating Na^+ at $d=2.5$ Å we find from our *ab initio* calculations that

$$\frac{e^2Q}{h}\langle q_{xx}\rangle-\frac{e^2Q}{h}\langle q_{xx}\rangle^{(\infty)}\approx-1.0\ \text{MHz},$$

$$\frac{e^2Q}{h}\langle q_{yy}\rangle-\frac{e^2Q}{h}\langle q_{yy}\rangle^{(\infty)}\approx 0.5\ \text{MHz}, \tag{23}$$

$$\frac{e^2Q}{h}\langle q_{zz}\rangle-\frac{e^2Q}{h}\langle q_{zz}\rangle^{(\infty)}\approx 0.5\ \text{MHz}.$$

The ratio of the these shifts are in agreement with the 2:-1:-1 ratio predicted by the point charge model.

1. Dependence on distance

In Fig. 5(a) and 5(b) is the dependence of C_q and η_q on the inverse cubed distance between the sodium cation and the bridging oxygen in the staggered $(OH)_3Si–O–Si(OH)_3$ cluster for Si–O–Si angles ranging between 120° and 180°. Clearly there is a systematic decrease in the magnitude of C_q and an increase in η_q with decreasing sodium-oxygen distance. At each distance this shift in both C_q and η_q appears to be nearly identical for all Si–O–Si angles between 120°

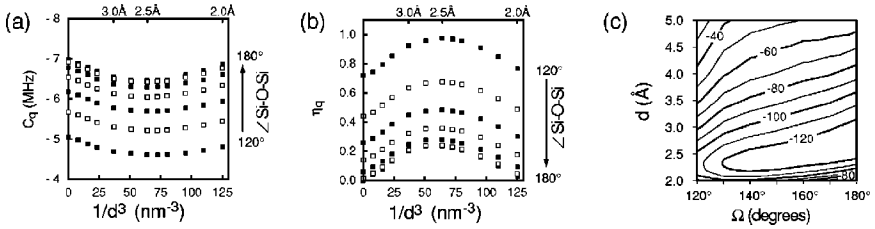

FIG. 5. *Ab initio* predicted values in (a) the ^{17}O quadrupolar coupling constant, C_q and (b) the ^{17}O quadrupolar asymmetry parameter, η_q, as a function of the inverse cubed sodium-cation oxygen distance and Si–O–Si angles ranging from 120° to 180°. In (c) is a contour plot of the *ab initio* predicted energy of the staggered $Na[(OH)_3Si–O–Si(OH)_3]^+$ molecule as a function of sodium cation-bridging oxygen distance and Si–O–Si angles. The energies plotted are relative to the energy of the cluster with a Si–O–Si angle of 180° at infinite cation separation.

and 180°. The initial decrease in C_q is linear with $1/d^3$ in agreement with Eqs. (15) and (18). The initial slopes yield Sternheimer anti-shielding factors ranging from $\gamma_\infty = -10.4$ at $\Omega = 120°$ to $\gamma_\infty = -12.1$ at $\Omega = 180°$. These values are reasonably close to the previously estimated value[22] of $\gamma_\infty = -28$. In addition, the initial slope of the $\eta_q C_q$ data (not shown) yielded γ_∞ values ranging from $\gamma_\infty = -4.9$ at $\Omega = 120°$ to $\gamma_\infty = -12.2$ at $\Omega = 180°$. As noted earlier, the dependence of γ_∞ on the Si–O–Si angle is not unexpected given the non-spherically symmetric electron distribution in the cluster. Note that the initial slopes from C_q and $\eta_q C_q$ give significantly different γ_∞ values at $\Omega = 120°$, yet are reasonably close at $\Omega = 180°$. This result is not surprising given the higher symmetry of the electron distribution in the $\Omega = 180°$ cluster.

As shown in Fig. 5(c), and as predicted in earlier *ab initio* work,[23] the cluster energy minimum occurs at lower Si–O–Si angles on approach of the alkali cation to the bridging oxygen. As the Si–O–Si angle increases from 120° to 180° the range of Na–O distances associated with these minimum energy clusters increase from 2.3 Å (82.2 nm^{-3}) to 2.7 Å (50 nm^{-3}), respectively. This range of Na–O distances is in agreement with the range of sodium–oxygen distances typically found in the first coordination sphere of bridging oxygen in crystalline sodium silicates. It is in this region that C_q and η_q also deviate from the $1/d^3$ point charge model dependence as a result of more substantial orbital interactions between sodium and oxygen, and become, somewhat fortuitously, effectively independent of the Na–O distance. Since the relative spacing of C_q and η_q values as a function of the Si–O–Si angle has remained essentially unchanged by the presence of the coordinating sodium cation the trends in C_q and η_q with Si–O–Si angle, as shown in Fig. 7, also remain relatively unchanged other than a systematic shift of C_q to lower magnitudes and η_q to higher values.

2. Dependence on cation nature

In Fig. 6 are the predicted C_q and η_q values as a function of alkali-bridging oxygen distance comparing the case of Li^+ and Na^+ coordination. Only data for the cluster with a Si–O–Si angle of 140° is presented. Consistent with the point charge approximation at large alkali-oxygen distances there are no differences between Na^+ and Li^+ for C_q and η_q. On closer approach deviations from the point charge model appear first for the larger sodium cation and then for the lithium cation. The Li^+ cation cluster reaches a minimum energy at a cation-oxygen distance near 1.9 Å as expected for lithium's smaller atomic radius. As with sodium, there is little variation in C_q and η_q due to variations with Li–O distance over the range of Li–O distances typically found in the first coordination sphere of the bridging oxygen in crystalline lithium silicates (i.e., near 2.0 Å). Also plotted in Fig. 7 are the trends in ^{17}O C_q and η_q with Si–O–Si angle for a Li^+ ($d = 2.0$ Å) coordinated oxygen. Again there is a systematic shift from the previously established dependence in ^{17}O quadrupolar coupling parameters on Si–O–Si angle with C_q decreased and η_q increased by amounts that clearly depend on the field strength of the coordinating alkali cation. In addition the nearly linear correlation between C_q and η_q is preserved with slight dependence of intercept on the cation field strength and an overall shift of the data to a lower C_q, higher η_q region. There is a departure from the trends in the case of the Li^+ cluster with a Si–O–Si angle of 120° that occurs because the ^{17}O efg PAS undergoes a shift in orientation with the z-axis of the efg lying perpendicular to the Li-O internuclear vector direction and in the plane that bisects the Si–O–Si angle.

Once again, it is useful to describe the dependences of C_q and η_q on Si–O–Si angle with analytical expressions. We can use the expression in Eq. (13) for $C_q^{(\infty)}$ and the point charge model as a basis for obtaining

$$C_q(\Omega) = a \cdot \left(\frac{1}{2} + \frac{\cos \Omega}{\cos \Omega - 1} \right)^{\alpha} - \Delta C_q^M , \tag{24}$$

where ΔC_q^M is the shift in C_q due to the presence of an alkali cation at its equilibrium distance. The solid lines in Fig. 7(a) represent the best fit of this function to the *ab initio* C_q data with the best fit parameters given in Table II. The two pa-

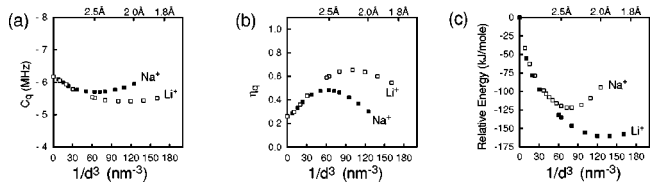

FIG. 6. Comparison of the *ab initio* predicted values in (a) the ^{17}O quadrupolar coupling constant, C_q, (b) the ^{17}O quadrupolar asymmetry parameter, η_q, and (c) the energy of the staggered $Li[(OH)_3Si–O–Si(OH)_3]^+$ and $Na[(OH)_3Si–O–Si(OH)_3]^+$ molecules as a function of the inverse cubed sodium cation-bridging oxygen distance for a Si–O–Si angle of 140°. The energies plotted in (c) are relative to the energy of the cluster with a Si–O–Si angle of 140° at infinite cation separation.

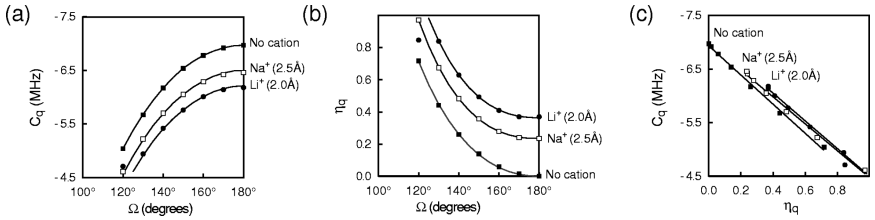

FIG. 7. Comparison of the *ab initio* predicted values in (a) the ^{17}O quadrupolar coupling constant, C_q, (b) the ^{17}O quadrupolar asymmetry parameter, η_q, and (c) the correlation between C_q and η_q for the bridging oxygen in the staggered $Li[(OH)_3Si{-}O{-}Si(OH)_3]^+$ and $Na[(OH)_3Si{-}O{-}Si(OH)_3]^+$ molecules as a function of the Si–O–Si angle. The sodium and lithium cations were positioned at the distance near the minimum cluster energy, that is, 2.5 Å and 2.0 Å, respectively. At a Si–O–Si angle of 120° the C_q and η_q deviate from the predicted trend due to a switch in efg PAS orientation. Solid lines in (a) and (b) represent the best fit curves of Eqs. (24) and (25), respectively, to the *ab initio* data. The solid lines in (c) are linear fits to the *ab initio* data. Best fit parameters for all curves are given in Table II.

rameters a and α in the Na^+ and Li^+ coordinated case are not significantly different from the case with no coordinating alkali cations; an indication of good qualitative agreement between the *ab initio* C_q data and the point charge model.

Although we could use the expression in Eq. (13) for $\eta_q^{(\infty)}$ with the point charge model to develop an analytical expression for η_q, the resulting expression is unwieldy and offers little insight. The approximate solution in Eq. (21) for η_q when $\phi=0°$ or 90°, however, can be used as a basis for proposing to simply add an offset term to our expression in Eq. (13) to obtain

$$\eta_q(\Omega)=b\cdot\left(\frac{1}{2}-\frac{\cos\Omega}{\cos\Omega-1}\right)^{\beta}+\Delta\eta_q^M. \tag{25}$$

Here the value of b is expected to be greater than in the case with no coordinating alkali cations, and the offset $\Delta\eta_q^M$ is expected to be on the order of $3\Delta C_q^M/C_q(\Omega)$. The solid lines in Fig. 7(b) represent the best fit of this function to the *ab initio* η_q data with the best fit parameters given in Table II. Since the offset is predicted to be dependent on Ω there are slightly greater deviations than expected for the best fit parameters β and b. Since the trends in C_q and η_q are essentially unchanged other than the constant shifts given in Table II, we would expect the linear correlation between C_q and η_q to be preserved as well, and this is seen in Fig. 7(c).

3. Dependence on orientation

While holding the sodium-bridging oxygen distance constant at 2.5 Å we varied the angle of the sodium–oxygen internuclear vector in the plane of the Si–O–Si angle [i.e., θ in Eq. (9)], and out of the Si–O–Si plane [i.e., ϕ in Eq. (9)] to study the effects of these changes on the bridging oxygen efg. The variations in cluster energy with θ and ϕ are shown in Fig. 8, and the variations of the ^{17}O efg tensor with θ and ϕ are shown in Figs. 9 and 10, respectively.

a. Rotation in the Si–O–Si plane: As seen in Fig. 8(a), outside a region of $\pm15°$ to $\pm35°$ depending on the Si–O–Si angle, there is a considerable energy barrier to moving the sodium–oxygen internuclear vector in the plane of the Si–O–Si angle. This is also consistent with the range of angles typically found near the bridging oxygen in crystalline sodium silicates. As shown in Fig. 9 there are relatively minor variations in both C_q and η_q with rotation of the sodium-oxygen internuclear vector in the plane of the the Si–O–Si angle. Interestingly, even though the $1/d^3$ dependence in Fig. 5 would indicate that at $d=2.5$ Å we are out of the point charge regime, it appears that the variations in C_q and η_q are still qualitatively consistent with the θ dependences given in Eqs. (15) and (21). ΔC_q^M values, however, were adjusted as a function of $\angle$Si–O–Si in order to obtain better agreement with the *ab initio* data. The variations in ΔC_q^M used for the C_q and η_q trends are given in the caption of Fig. 9. There are also relatively minor variations in the linear correlation between C_q and η_q, as seen in Fig. 5(c) which are also predicted by Eqs. (15) and (21).

Based on the high energy barrier associated with changing θ together with the small variations in both C_q and η_q observed in our *ab initio* data we conclude that the relationship of C_q and η_q to Si–O–Si angle given by Eqs. (24) and (25) would not be strongly affected by variations in θ.

b. Rotation out of the Si–O–Si plane: As seen in Fig. 8(b), the sodium–oxygen internuclear vector has effectively no energy barrier to rotation out of the plane of the Si–O–Si angle in contrast to the in-plane rotation (note scale of energy axes in Fig. 8). The *ab initio* predicted dependence of

TABLE II. Best fit parameters of Eqs. (24) and (25), and the linear fit to the *ab initio* predicted C_q and η_q data in the single coordinating alkali cation case. When using these parameters to predict the experimental C_q trends all ΔC_q^M values should be increased by 1.0 MHz. The C_q and η_q data for the Li^+ coordinated cluster with $\angle$Si–O–Si=120° were omitted when solving for these parameters.

	C_q dependence			η_q dependence			C_q, η_q correlation	
Cation	a (MHz)	α	ΔC_q^M (MHz)	b	β	$\Delta\eta_q^M$	slope (MHz)	intercept (MHz)
None	−6.97	1.78	0.00	5.03	1.09	0.000	2.72	−6.93
Na^+(d=2.5 Å)	−6.97	1.69	−0.51	6.13	1.18	0.235	2.51	−6.98
Li^+ (d=2.0 Å)	−6.97	1.70	−0.79	6.58	1.18	0.364	2.58	−7.08

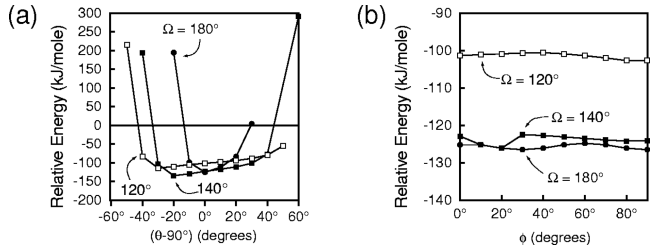

FIG. 8. *Ab initio* predicted energies for the staggered $Na[(OH)_3Si–O–Si(OH)_3]^+$ molecule as a function of (a) the angle between the Na-O internuclear vector and the plane perpendicular to the Si–O–Si plane and bisecting the Si–O–Si angle (i.e., $\theta-90°$), while keeping the Na-O internuclear vector in the plane of the Si–O–Si angle, and (b) the angle between the Na-O internuclear vector and the plane of the Si–O–Si angle (i.e., ϕ), while keeping the Na-O internuclear vector in the plane perpendicular to the Si–O–Si plane and bisecting the Si–O–Si angle. The energies plotted are relative to the energy of the cluster with a Si–O–Si angle of 180° at infinite cation separation.

the ^{17}O efg on ϕ is shown in Fig. 10. As predicted by Eq. (15) there is no variation in C_q with ϕ. The variation in η_q with ϕ also follow the trends predicted by Eq. (16) with the variations most pronounced at low Si–O–Si angles. Due to these strong variations in η_q with ϕ, the correlation between C_q and η_q deviates strongly from a linear correlation, with the greatest deviation occurring at $\phi=90°$. The variations in the (C_q, η_q) correlation for the *ab initio* data and predicted from the point charge model are shown in Fig. 10(c).

Clearly the variations in η_q with ϕ and the low energy barrier associated with moving the Na–O internuclear vector out of the Si–O–Si plane make η_q an unreliable parameter from which Ω, the Si–O–Si angle, can be determined. Fortunately, C_q is effectively independent of ϕ and can still act as a reliable probe of Ω. In principle, if both C_q and η_q could be measured, then both Ω and ϕ could be determined in the case of a single coordinating alkali cation.

C. The $M_2[(OH)_3SiOSi(OH)_3]$ cluster where $M=Li^+$ and Na^+

The effect of two coordinating alkali cations on the ^{17}O quadrupolar coupling parameters of the bridging oxygen were investigated by placing either a pair of Li^+ or Na^+ cations in the plane that is perpendicular to the Si–O–Si plane and bisects the Si–O–Si angle with each cation at an angle $\pm\Delta/2$, respectively, away from the bisector of the M–O–M angle as shown in Fig. 1(d). Once again, the optimized $(OH)_3Si–O–Si(OH)_3$ cluster geometry found for each Si–O–Si angle in the absence of alkali cations was used in the cluster containing the coordinating alkali cations. Although the cluster with the two cations is energetically unstable with respect to the cluster with infinite cation separation, we choose not to remedy this situation by coordinating an additional negative counter ion such as O^{2-} to the two cations since this would unnecessary complicate the comparison to the bridging oxygen efg tensor in the single cation clusters. Nonetheless, we performed additional calculations to determine the optimum Na–O distance in the $Na_2O[(OH)_3Si–O–Si(OH)_3]$ cluster for the $\angle$Si–O–Si of 140° and found a value of 2.23 Å, which is within 0.1 Å of the optimum distance found in the $Na[(OH)_3Si–O–Si(OH)_3]^+$ cluster. (The O^{2-} counter ion was constrained to lie in the Si–O–Si plane along the bisector of the Si–O–Si angle and above the two alkali cations.) In addition, the Na–O–Na angle in this optimized cluster was 88.3°.

Using the same assumptions of the last section we can predict variations in C_q, η_q, and efg PAS orientation with cation-oxygen distance and internuclear vector orientation in the case of two coordinating alkali cations by inserting Eq. (9) into Eqs. (10)–(12) to obtain

$$C_q(\Omega,d,\theta)\approx C_q^{(\infty)}(\Omega)+2\Delta C_q(d)\cdot(3\cos^2\theta-1), \tag{26}$$

$$\eta_q(\Omega,d,\theta,\phi)C_q(\Omega,d,\theta)\approx\sqrt{(6\Delta C_q(d)\sin^2\theta\cos 2\phi\cos\Delta+\eta_q^{(\infty)}(\Omega)C_q^{(\infty)}(\Omega))^2+(6\Delta C_q(d)\sin^2\theta\sin 2\phi\cos\Delta)^2}, \tag{27}$$

and

$$\tan 2\alpha\approx\frac{6\Delta C_q(d)\sin^2\theta\sin 2\phi\cos\Delta}{6\Delta C_q(d)\sin^2\theta\cos 2\phi\cos\Delta+C_q^{(\infty)}(\Omega)\eta_q^{(\infty)}(\Omega)}, \tag{28}$$

where Δ is the M–O–M angle, ϕ is the angle between the M–O–M bisector and Si–O–Si plane, and θ and d are assumed to be identical for both cations. Once again, there are a few noteworthy trends predicted by these equations:

(1) Equation (26) predicts that C_q is generally independent of ϕ and Δ, and with d held constant that the trend in C_q with Ω is shifted by a constant offset that is modulated by $(3\cos^2\theta-1)$ and is twice the magnitude of the offset in the case of a single coordinating alkali cation.

(2) If $\Delta=90°$ or 270° then

$$\eta_q(\Omega,d,\theta,\phi)=\eta_q^{(\infty)}(\Omega)\left(\frac{C_q^{(\infty)}(\Omega)}{C_q(\Omega,d,\theta)}\right), \tag{29}$$

and the trend in η_q is simply scaled and is generally independent of ϕ.

(3) In the special case where $\eta_q^{(\infty)}(\Omega)=0$ (i.e., $\angle$Si–O–Si $=180°$) Eq. (27) gives an expression for η_q,

$$\eta_q(\Omega,d,\theta,\phi)\approx 3\left(\frac{\Delta C_q(d)}{C_q(\Omega,d,\theta)}\right)\sin^2\theta\cos\Delta, \tag{30}$$

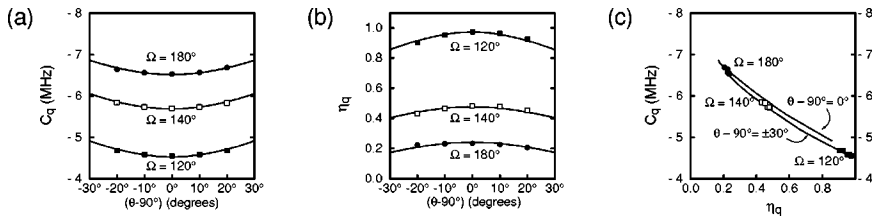

FIG. 9. *Ab initio* predicted values in (a) the ^{17}O quadrupolar coupling constant, C_q, (b) the ^{17}O quadrupolar asymmetry parameter, η_q, and (c) the correlation between C_q and η_q for the bridging oxygen in the staggered $Na[(OH)_3Si–O–Si(OH)_3]^+$ molecule as a function of the angle between the Na-O internuclear vector and the plane perpendicular to the Si–O–Si plane and bisecting the Si–O–Si angle (i.e., $\theta-90°$), while keeping the Na-O internuclear vector in the plane of the Si–O–Si angle. Lines in (a) represent the best fit to Eq. (15) with $\Delta C_q^M = 0.57$, 0.54, and 0.53 for $\Omega = 120°$, 140°, and 180°, respectively. Lines in (b) represent the best fit to Eq. (21) with $\Delta C_q^M = 0.25$, 0.36, and 0.52 for $\Omega = 120°$, 140°, and 180°, respectively. Lines in (c) represent the variation in the correlation between C_q and η_q for $(\theta-90°)=0°$ and $(\theta-90°)=\pm 30°$ predicted by Eqs. (15) and (21).

that is generally independent of ϕ. In addition, Eq. (28) also reduces to $\tan 2\alpha = \tan 2\phi$, indicating that the bisector of the M–O–M angle defines the direction of the x-axis of the efg PAS.

(4) If $\phi = 0°$ or 90° then Eq. (27) gives an expression for η_q,

$$\eta_q(\Omega,d,\theta,\phi) \approx \eta_q^{(\infty)}(\Omega)\left(\frac{C_q^{(\infty)}(\Omega)}{C_q(\Omega,d,\theta)}\right) + 6\left(\frac{\Delta C_q(d)}{C_q(\Omega,d,\theta)}\right)\sin^2\theta\cos\Delta, \tag{31}$$

that predicts that the trend in η_q with Ω is simply scaled and shifted by a constant times $\sin^2\theta\cos\Delta$.

(5) In the case where $\phi = 0°$ and $\theta = 90°$, as shown in Fig. 1(d), we obtain the following expressions from Eq. (8):

$$\frac{e^2Q}{h}\langle q_{xx}\rangle = \frac{e^2Q}{h}\langle q_{xx}\rangle^{(\infty)} + \Delta C_q(d)\cdot(1+3\cos\Delta),$$

$$\frac{e^2Q}{h}\langle q_{yy}\rangle = \frac{e^2Q}{h}\langle q_{yy}\rangle^{(\infty)} + \Delta C_q(d)\cdot(1-3\cos\Delta), \tag{32}$$

$$\frac{e^2Q}{h}\langle q_{zz}\rangle = \frac{e^2Q}{h}\langle q_{zz}\rangle^{(\infty)} - 2\Delta C_q(d).$$

(a) Near $\Delta = 90°$ these equations predict that upon approach of the cations $\langle q_{xx}\rangle$, $\langle q_{yy}\rangle$, and $\langle q_{zz}\rangle$ decrease in magnitude with $\langle q_{zz}\rangle$ decreasing at a rate twice that of $\langle q_{xx}\rangle$ and $\langle q_{yy}\rangle$. As a point of reference, for two coordinating Na^+ cations at $d = 2.5$ Å and $\Delta = 90°$ we find from our *ab initio* calculations that

$$\frac{e^2Q}{h}\langle q_{xx}\rangle - \frac{e^2Q}{h}\langle q_{xx}\rangle^{(\infty)} \approx -0.5 \text{ MHz},$$

$$\frac{e^2Q}{h}\langle q_{yy}\rangle - \frac{e^2Q}{h}\langle q_{yy}\rangle^{(\infty)} \approx -0.5 \text{ MHz}, \tag{33}$$

$$\frac{e^2Q}{h}\langle q_{zz}\rangle - \frac{e^2Q}{h}\langle q_{zz}\rangle^{(\infty)} \approx 1.0 \text{ MHz}.$$

The ratio of the these shifts are in agreement with the those predicted by the point charge model.

(b) Near $\Delta = 109.5°$ these equations predict that upon approach of the cations $\langle q_{xx}\rangle$ remains constant in magnitude while $\langle q_{yy}\rangle$ decreases in magnitude at the same rate as $\langle q_{zz}\rangle$. However, if $|\langle q_{yy}\rangle|$ becomes less than $|\langle q_{xx}\rangle|$, then $\langle q_{xx}\rangle$ and $\langle q_{yy}\rangle$ swap definitions and $\langle q_{xx}\rangle$ decreases in magnitude upon approach of the cation while $\langle q_{yy}\rangle$ remains constant. Similarly, near $\Delta = 70.5°$ these equations predict that upon approach of the cations $\langle q_{yy}\rangle$ remains constant in magnitude while $\langle q_{xx}\rangle$ decreases in magnitude at the same rate as $\langle q_{zz}\rangle$.

(c) Near $\Delta = 180°$ these equations predict the greatest changes in $\langle q_{xx}\rangle$ and $\langle q_{yy}\rangle$ upon approach of the cations, with $\langle q_{xx}\rangle$ increasing at the same rate that $\langle q_{zz}\rangle$ is decreasing, and $\langle q_{yy}\rangle$ decreasing at twice the rate of $\langle q_{zz}\rangle$.

A comparison of the trends in ^{17}O quadrupolar coupling parameters for the bridging oxygen as a function of Si–O–Si angle in the case of zero, one, and two coordinating alkali

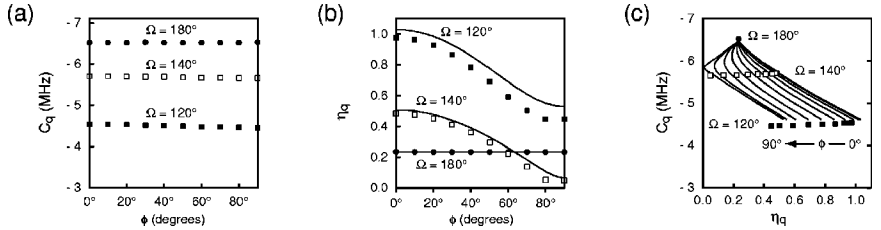

FIG. 10. *Ab initio* predicted values in (a) the ^{17}O quadrupolar coupling constant, C_q, (b) the ^{17}O quadrupolar asymmetry parameter, η_q, and (c) the correlation between C_q and η_q for the bridging oxygen in the staggered $Na[(OH)_3Si–O–Si(OH)_3]^+$ molecule as a function of the angle between the Na–O internuclear vector and the plane of the Si–O–Si angle, while keeping the Na–O internuclear vector in the plane perpendicular to the Si–O–Si plane and bisecting the Si–O–Si angle. Lines in (b) represent the best fit to Eqs. (15) and (16) with $\Delta C_q^M = 0.38$, 0.39, and 0.50 for $\Omega = 120°$, 140°, and 180°, respectively. Lines in (c) represent the variation in the correlation between C_q and η_q predicted by Eqs. (15) and (16) as a function of Ω and ϕ.

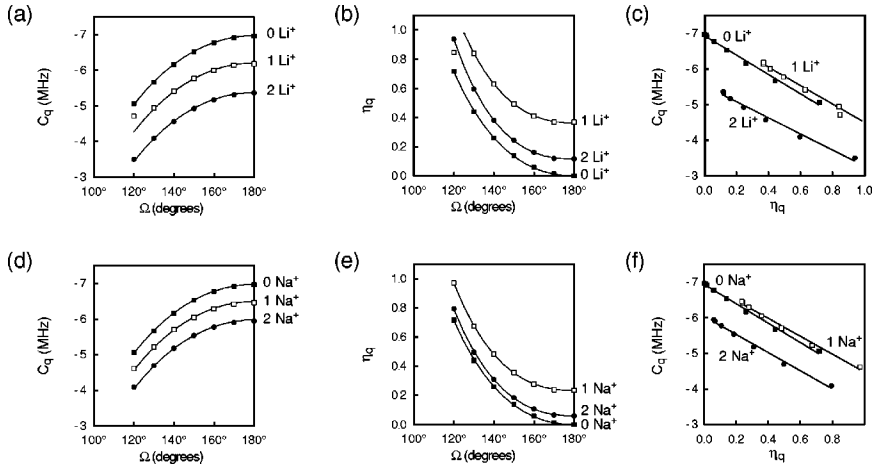

FIG. 11. Comparison of the *ab initio* predicted values in (a,d) the ^{17}O quadrupolar coupling constant, C_q, (b,e) the ^{17}O quadrupolar asymmetry parameter, η_q, and (c,f) the correlation between C_q and η_q for the bridging oxygen in the staggered Li_n $[(OH)_3Si–O–Si(OH)_3]^{n+}$ ($d=2.0$ Å) and Na_n $[(OH)_3Si–O–Si(OH)_3]^{n+}$ ($d=2.5$ Å) molecules as a function of Si–O–Si angle for increasing number of alkali coordinating near the bridging oxygen. In the two cation clusters we have set $\Delta=90°$. Solid lines in (a), (b), (d) and (e) represent the best fit curves of Eqs. (24), (25), and (34), and solid lines in (c) and (f) are linear fits to the *ab initio* data. Best fit parameters for all curves are given in Tables II and III.

cations is shown in Figs. 11(a)-11(c) for the Li_2 $[(OH)_3SiOSi(OH)_3]^{2+}$ cluster and in Figs. 11(d)–11(f) for the Na_2 $[(OH)_3SiOSi(OH)_3]^{2+}$ cluster. For C_q the effect of a second cation is cumulative with the magnitude of the additive shift dependent on the cation field strength. As predicted by Eq. (26) this shift is twice that of the single cation in both the Li^+ and Na^+ case. The effect of two cations on the asymmetry parameter, however, is markedly different than in the single cation case. The presence of two cations with $\Delta=90°$ only slightly shifts the asymmetry parameter to higher values in comparison to the large shift induced by a single coordinating cation. Again, this is predicted in the $\Delta=90°$ case where Eq. (27) reduces to Eq. (29). As seen in Figs. 11(c) and 11(f) the nearly linear correlation between C_q and η_q is preserved in the two cation case with little change in slope but a significant change in intercept. This change in correlation intercept may prove useful as a means of experimentally distinguishing different coordination environments of the bridging oxygen.

To describe the dependences of C_q and η_q on Si–O–Si angle we have used the following analytical expressions:

$$C_q = a\cdot\left(\frac{1}{2}+\frac{\cos\Omega}{\cos\Omega-1}\right)^{\alpha}-2\Delta C_q^M, \quad \text{and}$$

$$\eta_q = b\cdot\left(\frac{1}{2}-\frac{\cos\Omega}{\cos\Omega-1}\right)^{\beta}+\Delta\eta_q^M. \tag{34}$$

The solid lines in Figs. 11(a), 11(b), 11(d), and 11(e) represent the best fit of these two functions to the *ab initio* derived C_q and η_q data with the best fit parameters given in Table III.

Dependence on orientation. In the case of two coordinating akali cations we also investigated the dependence of C_q and η_q on the rotation of the M–O–M bisector out of the Si–O–Si plane. While holding Δ constant the changes in cluster energy with variations in ϕ (data not shown) are negligible as was the case with the single coordinating alkali cation. While holding ϕ constant the changes in cluster energy with variations in Δ are substantial (from 172 kJ at $\Delta=75°$ to 65.3 kJ at $\Delta=120°$). In the absence of a counter ion such as O^{2-}, however, this energy difference is not a realistic basis for predicting the M–O–M angle.

When the two cations are both coordinated to the same O^{2-} counter ion our *ab initio* calculations predicted an M–O–M angle near 90°. The *ab initio* predicted dependence of the ^{17}O C_q and η_q on ϕ for $\Delta=90°$ is shown in Figs. 12(a) and 12(b) for the Na_2 $[(OH)_3Si–O–Si(OH)_3]^{2+}$ cluster. As predicted by Eq. (26) there is no variation in C_q with ϕ, and as predicted by Eq. (29) there is little to no variation in η_q with ϕ. The variations in the correlation between C_q and η_q for the *ab initio* data and predicted from the point charge model are shown in Fig. 12(c). Because of the near invariance in both C_q and η_q with ϕ the correlation between

TABLE III. Best fit parameters for Eq. (34), and the linear fit to the C_q, η_q *ab initio* data in the case of two coordinating alkali cation case. When using these parameters to predict the experimental C_q trends all ΔC_q^M values should be increased in magnitude by 1.0 MHz.

	C_q dependence			η_q dependence			C_q, η_q correlation	
Cation	a (MHz)	α	ΔC_q^M (MHz)	b	β	$\Delta\eta_q^M$	slope (MHz)	intercept (MHz)
Na^+ ($d=2.5$ Å)	−6.97	1.71	−0.51	6.03	1.18	0.061	2.54	−6.03
Li^+ ($d=2.0$ Å)	−6.97	1.71	−0.81	7.46	1.23	0.116	2.26	−5.53

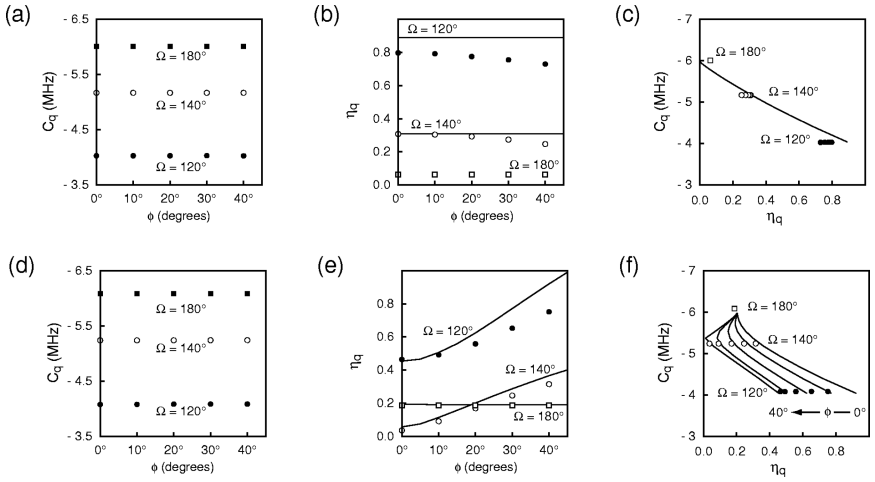

FIG. 12. *Ab initio* predicted values in (a), (d) the ^{17}O quadrupolar coupling constant, C_q, (b), (e) the ^{17}O quadrupolar asymmetry parameter, η_q, and (c), (f) the correlation between C_q and η_q for the bridging oxygen in the staggered $Na_2[(OH)_3Si{-}O{-}Si(OH)_3]^{2+}$ molecule as a function of Si–O–Si angle and the angle between the Na–O–Na bisector and the plane of the Si–O–Si angle, while keeping the two sodium cations in the plane bisecting the Si–O–Si angle. Data in (a), (b), (c) were calculated for $\Delta=90°$ and (d), (e), (f) for $\Delta=120°$. Lines in (b), (d) represent the best fit to Eqs. (26) and (27) with $\Delta C_q^M = 0.57$, 0.43, and 0.38 ($\Delta=120°$ only) for $\Omega=120°$, 140°, and 180°, respectively. Lines in (c), (f) represent the variation in the correlation between C_q and η_q predicted by Eqs. (26) and (27) as a function of Ω and ϕ.

C_q and η_q deviates only slightly from a linear correlation.

The *ab initio* predicted dependence of the ^{17}O C_q and η_q on ϕ for $\Delta=120°$ is shown in Figs. 12(d) and 12(e). Once again, there is no variation in C_q with ϕ or Δ as predicted by Eq. (26). For $\Delta=120°$ the point charge model predicts stronger variations in η_q with ϕ, with the most pronounced variations occurring at low Si–O–Si angles. The variations in the correlation between C_q and η_q for the *ab initio* data and predicted from the point charge model are shown in Fig. 10(g). As was the case in the single coordinating alkali cation case, there will be increasing deviations from the linear correlation with increasing ϕ.

Clearly the variations in η_q with ϕ when $\Delta\neq 90$ and the low energy barrier associated with moving the Na–O internuclear vector out of the Si–O–Si plane once again make η_q somewhat of an unreliable parameter from which Ω, the Si–O–Si angle, can be determined. As in the single coordinating alkali cation case, however, C_q is effectively independent of ϕ and can still act as a reliable probe of Ω. In the absence of an η_q dependence on ϕ (i.e. when $\Delta=90°$), one could use the intercept of the linear correlation between C_q and η to distinguish between one and two alkali cations coordinating the bridging oxygen as seen in Fig. 11 and indicated in Tables II and III.

D. The $M_n[(OH)_3SiOSi(OH)_3]$ cluster where $n=3$ or 4

Although we did not pursue *ab initio* calculations on clusters containing three or more coordinating alkali cations we can predict the behavior of C_q and η_q on the basis of our point charge model. If we assume that all coordinating alkali cations have the same θ value and are spaced around the bridging oxygen such that $\Delta=\angle M_1{-}O{-}M_2=\angle M_2{-}O{-}M_3=\angle M_3{-}O{-}M_4$ then our starting point for the point charge model in the three coordinating alkali cation case is

$$\langle R_{2,m}(\Omega)\rangle=\langle\rho_{2,m}^{(\infty)}(\Omega)\rangle+(1-\gamma_\infty)\frac{Ze}{d^3}\sqrt{\frac{4\pi}{5}}Y_{2,m}(\theta,\phi)\times\left\{2\cos\left(\frac{m\Delta}{2}\right)+1\right\},\tag{35}$$

and in the four coordinating alkali cation case is

$$\langle R_{2,m}(\Omega)\rangle=\langle\rho_{2,m}^{(\infty)}(\Omega)\rangle+(1-\gamma_\infty)\frac{Ze}{d^3}\sqrt{\frac{4\pi}{5}}Y_{2,m}(\theta,\phi)\times\left\{2\cos\left(\frac{m\Delta}{2}\right)+2\cos\left(\frac{3m\Delta}{2}\right)\right\}.\tag{36}$$

C_q is derived from the $m=0$ element and the equations above predict that C_q will vary linearly with alkali cation coordination number. Assuming that the three and four alkali cations would coordinate with θ near 90° (i.e., all cations near the plane that is perpendicular to the Si–O–Si plane and bisects the Si–O–Si angle), then we would conclude that C_q is systematically decreased with increasing number of coordinating alkali cations, and would be relatively insensitive to orientational changes (i.e. ϕ and Δ) of the coordinating alkali cations. Thus, given the number of coordinating alkali cations C_q would still serve as a reliable probe of the Si–O–Si bond angle.

η_q is derived from $m=\pm 2$ elements and in general would depend on the relative (Δ) and overall (ϕ) orientation of the coordinating alkali cations in a manner that is similar to the single coordinating alkali cation case. However, the variations in η_q due to changing orientation of coordinating alkali cations are expected to be smaller in magnitude compared to the single coordinating alkali cation case, and to have no variations due to changing orientation in the limiting cases of $\Delta=120°$ and 90° for the three and four coordinating

alkali cation cases, respectively. In general, η_q may have limited utility as a probe of the Si–O–Si bond angle, but could serve as a probe of the orientational configuration of the coordinating alkali cations. If the alkali cations were spaced such that η_q is independent of the orientation of the coordinating alkali cations, then, as noted in the last section, the intercept of the linear correlation between C_q and η can be used to determine the total number of coordinating alkali cations surrounding the bridging oxygen.

IV. SUMMARY AND CONCLUSIONS

We have performed *ab initio* calculations on what we consider to be the simplest cluster molecules needed to reproduce the dependence of the experimentally measured ^{17}O quadrupolar coupling parameters on the local structure around the bridging oxygen in the case of alkali silicates. We have also found that a point charge model can be used to derive approximate expressions to describe the dependence of the ^{17}O electric field gradient tensor on the orientation of the alkali cation-bridging oxygen internuclear vector(s). Based on these results we predict that the ^{17}O quadrupolar coupling constant, C_q, can still act as a reliable probe of the Si–O–Si angle with the previously established trend in C_q with Si–O–Si angle systematically shifted to lower magnitudes with increasing number and field strength of coordinating alkali cations. In general, C_q is relatively insensitive to orientational changes in the coordinating alkali cation-oxygen bridging internuclear vector. In contrast, the bridging oxygen ^{17}O quadrupolar coupling asymmetry parameter, η_q, is sensitive to the orientational changes in the coordinating alkali cation-bridging oxygen internuclear vector(s) and thus may no longer act as a reliable probe of Si–O–Si angle in the presence of coordinating alkali cations. Under specific assumptions for coordinating alkali cation orientations the previously established trend in η_q with Si–O–Si angle is systematically shifted to higher values by the presence of a single coordinating alkali cation, and only slightly shifted to higher values by the presence of two or more coordinating alkali cations. As with the quadrupolar coupling constant, the extent of the shift in asymmetry parameter increases with increasing field strength of the coordinating alkali cation(s). In the absence of an η_q dependence on the orientation of the coordinating alkali cation-bridging oxygen internuclear vector the intercept of the linear correlation between C_q and η can be used to determine the total number of coordinating alkali cations surrounding the bridging oxygen.

We expect that coordinating alkali cations with larger radii and lower field strengths would result in smaller overall shifts in the previously established C_q and η_q trends with Si–O–Si angle. In contrast, for network modifying cations of smaller radius and higher field strength, such as Mg^{2+} or Be^{2+}, we also expect that these cations would so strongly affect the efg of the bridging oxygen that a change in its PAS is likely and thus the trends of bridging oxygen efg with Si–O–Si would be considerably different from the trends presented here. Further *ab initio* investigations on both types of situations is in progress.

Unfortunately, given the paucity of experimental ^{17}O solid-state NMR data a comparison of experimental ^{17}O bridging oxygen data in crystalline lithium and sodium silicates to our *ab initio* derived trends is problematic. Future experimental ^{17}O NMR work in these and related systems of known structure will be invaluable in fine tuning our correlations, and improving the quality of structural information available through ^{17}O solid-state NMR.

ACKNOWLEDGMENTS

We thank Alex Klymachyov for computational assistance. P.J.G. acknowledges support from the National Science Foundation (No. CHE-9501872) and the Donors of The Petroleum Research Fund, administered by the American Chemical Society.

[1] A. Samoson, E. Lippmaa, and A. Pines, Mol. Phys. **65**, 1013 (1988).
[2] A. Llor and J. Virlet, Chem. Phys. Lett. **152**, 248 (1988).
[3] B. F. Chmelka, K. T. Mueller, A. Pines, J. Stebbins, Y. Wu, and J. W. Zwanziger, Nature (London) **339**, 42 (1989).
[4] K. T. Mueller, B. Q. Sun, G. C. Chingas, J. W. Zwanziger, T. Terao, and A. Pines, J. Magn. Reson. **86**, 470 (1990).
[5] P. J. Grandinetti, in *Encyclopedia of Nuclear Magnetic Resonance* edited by David M. Grant and Robin K. Harris (Wiley, New York, 1995), p. 1768.
[6] L. Frydman and J. S. Harwood, J. Am. Chem. Soc. **117**, 5367 (1995).
[7] J. A. Tossell and P. Lazzeretti, Chem. Phys. Lett. **112**, 205 (1987).
[8] J. A. Tossell and P. Lazzeretti, Phys. Chem. Miner. **15**, 564 (1988).
[9] C. G. Lindsay and J. A. Tossell, Phys. Chem. Miner. **18**, 191 (1991).
[10] P. J. Grandinetti, J. H. Baltisberger, U. Werner, A. Pines, I. Farnan, and J. F. Stebbins, J. Phys. Chem. **99**, 12341 (1995).
[11] I. Farnan, P. J. Grandinetti, J. H. Baltisberger, J. F. Stebbins, U. Werner, M. A. Eastman, and A. Pines, Nature (London) **358**, 31 (1992).
[12] H. Maekawa, P. Florian, D. Massiot, H. Kiyono, and M. Nakamura, J. Phys. Chem. **100**, 5525 (1996).
[13] A factor of 2 was inadvertently omitted in these relationships in our earlier paper (Ref. 10). This error, however, was not propagated into any of the later expressions, and had no bearing on any of the discussions or conclusions in that paper.
[14] GAUSSIAN 94, Revision b.3., M. J. Frisch, G. W. Trucks, H. B. Schlegel, P. M. W. Gill, B. G. Johnson, M. A. Robb, J. R. Cheeseman, T. Keith, G. A. Petersson, J. A. Montgomery, K. Raghavachari, M. A. Al-Laham, V. G. Zakrzewski, J. V. Ortiz, J. B. Foresman, C. Y. Peng, P. Y. Ayala, W. Chen, M. W. Wong, J. L. Andres, E. S. Replogle, R. Comperts, R. L. Martin, D. J. Fox, J. S. Binkley, D. J. Defrees, J. Baker, J. P. Stewart, M. Head-Gordon, C. Gonzalez, and J. A. Pople, Gaussian, Inc., Pittsburgh, Pennyslvania, 1995.
[15] R. Sternheimer, Phys. Rev. **86**, 316 (1952).
[16] E. A. C. Lucken, *Nuclear Quadrupole Coupling Constants* (Academic, London, 1969).
[17] G. V. Gibbs, Am. Mineral. **67**, 421 (1982).
[18] X. Xue, J. F. Stebbins, and M. Kanzaki, Am. Mineral. **79**, 31 (1994).
[19] N. Janes and E. Oldfield, J. Am. Chem. Soc. **108**, 5743 (1986).
[20] C. H. Townes and B. P. Dailey, J. Chem. Phys. **17**, 782 (1949).
[21] U. Sternberg, Solid State Nucl. Magn. Reson. **2**, 181 (1993).
[22] G. Burns and E. G. Wikner, Phys. Rev. **121**, 155 (1961).
[23] K. L. Geisinger, G. V. Gibbs, and A. Navrotsky, Phys. Chem. Miner. **11**, 266 (1985).